Investigation of polymer electrolyte membrane chemical degradation and degradation mitigation using in situ fluorescence spectroscopy

Venkateshkumar Prabhakaran, Christopher G. Arges, and Vijay Ramani[1]

Department of Chemical and Biological Engineering, Illinois Institute of Technology, 10 West 33rd Street, Chicago, IL 60616

Edited by Alexis T. Bell, University of California, Berkeley, CA, and approved November 22, 2011 (received for review September 6, 2011)

A fluorescent molecular probe, 6-carboxy fluorescein, was used in conjunction with in situ fluorescence spectroscopy to facilitate real-time monitoring of degradation inducing reactive oxygen species within the polymer electrolyte membrane (PEM) of an operating PEM fuel cell. The key requirements of suitable molecular probes for in situ monitoring of ROS are presented. The utility of using free radical scavengers such as CeO_2 nanoparticles to mitigate reactive oxygen species induced PEM degradation was demonstrated. The addition of CeO_2 to uncatalyzed membranes resulted in close to 100% capture of ROS generated in situ within the PEM for a period of about 7 h and the incorporation of CeO_2 into the catalyzed membrane provided an eightfold reduction in ROS generation rate.

fuel cells | Nafion® degradation | hydroxyl radicals | hydroperoxyl radicals | miniature fluorescence probe

Hydrogen/air (H_2/air) polymer electrolyte membrane (PEM) fuel cells possess high efficiency and modularity. However, significant technical advances are required to facilitate fuel cells' commercialization and widespread use in targeted applications in the automotive, portable power, and military sectors. A key technological issue that remains to be addressed is component durability under an array of adverse operating conditions. The ion-exchange membrane in a PEM fuel cell is one of the components whose limited long-term durability is of concern. The PEM undergoes mechanical, thermal, and chemical degradation during fuel cell operation (1–8). The chemical degradation process that takes place in a H_2/O_2 PEM fuel cell is attributed to reactive oxygen species (ROS) that are generated in situ through both chemical and electrochemical pathways during fuel cell operation. Hydrogen peroxide (H_2O_2) is an ROS and is often an intermediate formed in both pathways and is known to form free radical ROS in the presence of transition metal ions via the Fenton mechanism (9–12). These free radical ROS, namely hydroxyl and hydroperoxyl radicals, are amongst the strongest oxidizing agents known. ROS initiate oxidative degradation of both the PEM backbone and the side chains that contain ionic groups that are essential for ion conduction (13–16). The adverse consequences of these degradation modes (e.g., membrane thinning, pin-hole formation, and loss of ionic conductivity) eventually contribute to catastrophic cell and stack failure. Complete elimination of ROS generation and PEM chemical degradation, while a worthy goal, is difficult due to constraints in terms of membrane materials, choice of fuel and oxidant, and fuel cell operating conditions. Therefore, it is imperative to develop effective mitigation strategies that minimize the rate and extent of PEM degradation.

Prior to proposing an effective mitigation strategy, it is essential to quantify the rate of ROS generation within the PEM during fuel cell operation. However, detecting the presence of ROS within the PEM of an operating fuel cell is an extremely difficult proposition because free radical ROS (e.g., hydroxyl and hydroperoxyl radicals) have half-lives on the order of 10^{-9} s (17). A survey of the literature suggests that ROS-induced PEM degradation has largely been studied through indirect methods, where the PEM degradation products were assayed from the effluent water emanating from the fuel cell (18, 19) or the PEMs themselves were examined in postmortem studies (14, 20). These ex situ approaches often required extensive sample preparation before analytical measurement, and did not yield real-time data. It was therefore difficult to extract a strong causal relationship between fuel cell operating parameters, ROS generation rates, and ROS-induced chemical degradation. The presence of ROS in PEM fuel cells has been directly identified by electron paramagnetic resonance (EPR) measurements (21–24). However, these measurements are limited to cells that fit within the EPR probe and cannot be translated to subscale or larger scale cells operating under realistic conditions. Nosaka and coworkers reported the indirect measurement of ROS generation rates using fluorescence spectroscopy, where a fluorescent molecular probe, coumarin, was incorporated into the fuel cell and the probe was shown to be sensitive to ROS (25). Nosaka, et.al.'s experimental setup involved placing a solution of the fluorescence agent adjacent to the fuel cell electrodes, where they monitored the fluorescence of this solution ex situ. There are many reports from the chemical biology literature that describe the use of fluorescence spectroscopy to indirectly monitor ROS (25–31). In this paper, we improve upon on Nosaka, et.al.'s concept of indirectly measuring ROS via fluorescence spectroscopy by developing an in situ fluorescence probe that monitors the generation of ROS in real-time during fuel cell operation. The operational concept presented in this paper stems from the work of Patil, et al., who developed and employed an in situ fluorescence technique to monitor water content within the PEM during fuel cell operation (32). The present work extends this concept to the much more challenging task of monitoring the generation of unstable and short-lived ROS.

In this study, 6-carboxy fluorescein (6CFL) was selected as the fluorescent molecular probe because: (*i*) 6CFL yielded a strong fluorescence signal in acidic media. (*ii*) it possessed a sufficiently large difference between its excitation and emission wavelengths, thereby affording good resolution. In a typical fluorescence spectrometer, good resolution between the excitation and emission wavelengths is not necessarily required because the fluorescence signal is collected at an angle of 90° to the incidence of the excitation light source. However, the detector in the miniature bifurcated optical probe used for in situ experiments in this study (discussed in greater detail later in the paper) senses light from the excitation light source in addition to the fluorescence response of the molecular probe. Collection of the fluorescence signal without interference from the excitation light source is

Author contributions: V.P., C.G.A., and V.R. designed research; V.P. and C.G.A. performed research; V.P., C.G.A., and V.R. contributed new reagents/analytic tools; V.P., C.G.A., and V.R. analyzed data; and V.P., C.G.A., and V.R. wrote the paper.

The authors declare no conflict of interest.

This article is a PNAS Direct Submission.

[1]To whom correspondence should be addressed. E-mail: ramani@iit.edu.

This article contains supporting information online at www.pnas.org/lookup/suppl/doi:10.1073/pnas.1114672109/-/DCSupplemental.

difficult in the constrained environment of a fuel cell membrane. (*iii*) 6CFL demonstrated high sensitivity to free radical ROS and its fluorescence signal was measurably attenuated in the presence of these species (33, 34). The signal was unchanged in the presence of hydrogen, oxygen, water, or H_2O_2 alone. (*iv*) 6CFL was observed to have good compatibility with Nafion®, the PEM used in this work. Fluorescein (FL) was also evaluated as a candidate molecular probe because it was sensitive to ROS; however, 6CFL exhibited substantially more robust properties in the context of the experiments performed. Therefore, all in situ results reported in this paper were obtained with 6CFL as the fluorescent molecular probe.

Results and Discussion

Ex Situ Fluorescence Experiments. The suitability of the molecular probe was assessed by performing ex situ experiments. The setup employed for ex situ fluorescence experiments is depicted in Fig. 1.

In addition to quantifying the rate of ROS generation in an operating fuel cell, the fluorescence spectroscopy technique was also used to evaluate the efficacy of incorporating a free radical scavenger (FRS) within the PEM as a potential degradation mitigation strategy. The FRS selected was cerium (IV) oxide (CeO_2) nanoparticles, and the CeO_2 nanoparticles were evaluated in both in situ and ex situ experiments. The use of cerium oxide as a FRS has been previously reported in in situ and ex situ studies, where it has been demonstrated to be regenerative in acidic media (19, 35–37).

The radical scavenging mechanism of cerium (IV) oxide is illustrated in Fig. 2. It is important to point out that CeO_2 is completely regenerative at the end of the scavenging cycle (19, 37). As shown in Fig. 1, ex situ experiments were performed in a semibatch style reactor to assess the change in fluorescence. The molecular probe, either FL or 6CFL, was dissolved in an aqueous solution containing either iron (III) or cobalt (II) transition metal ions. Aliquots of H_2O_2 were then added into the well-stirred reactor. The transition metal ions catalyzed the conversion of H_2O_2 to hydroxyl and hydroperoxyl radicals within the reactor (Fenton mechanism). The decrease in fluorescence signal intensity was evaluated as a function of H_2O_2 concentration. A linear relationship was observed between the reduction in fluorescence signal intensity and the amount of H_2O_2 (quencher-C_Q) added to the reactor, suggesting that the system obeyed the Stern-Volmer relationship given in Eq. **1**.

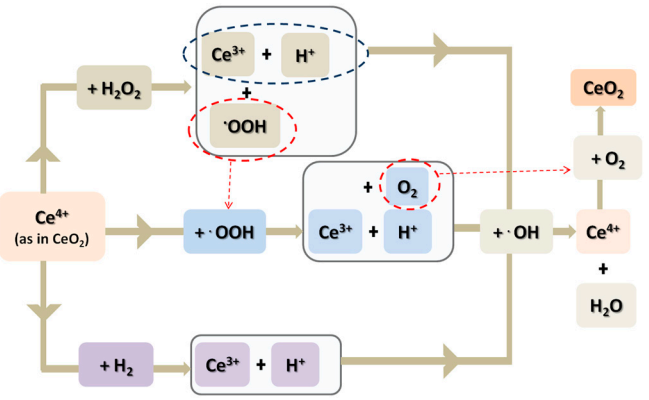

Fig. 2. Cerium (IV) oxide radical scavenging mechanism.

$$\frac{I_o}{I} = 1 + K_{SV}C_Q \qquad [1]$$

I_o—Initial fluorescence intensity without quencher, I—Fluorescence intensity at any time after quencher addition, C_Q—Quencher concentration, and K_{SV}—Stern-Volmer quenching constant. It is important to note that the quenched fluorescence intensity value was recorded only after the system achieved equilibrium, as determined by monitoring the change in fluorescence as function of time upon addition of H_2O_2. For each H_2O_2 addition, the system achieved equilibrium in less than 2 min. The experiment was repeated without transition metal ions (which are essential for free radical ROS generation) and it was shown that FL and 6CFL were only sensitive towards free radical ROS, and not towards H_2O_2.

In early experiments, FL was selected as the molecular probe without gauging its suitability in acidic media. Ex situ experiments using FL were performed with various amounts of CeO_2 nanoparticles suspended in solution to verify efficacy of CeO_2 as a FRS. These experiments were carried out at neutral pH, where FL was effective (see *SI Text*, pp. 1, 2, and 5). Fig. 3 shows the

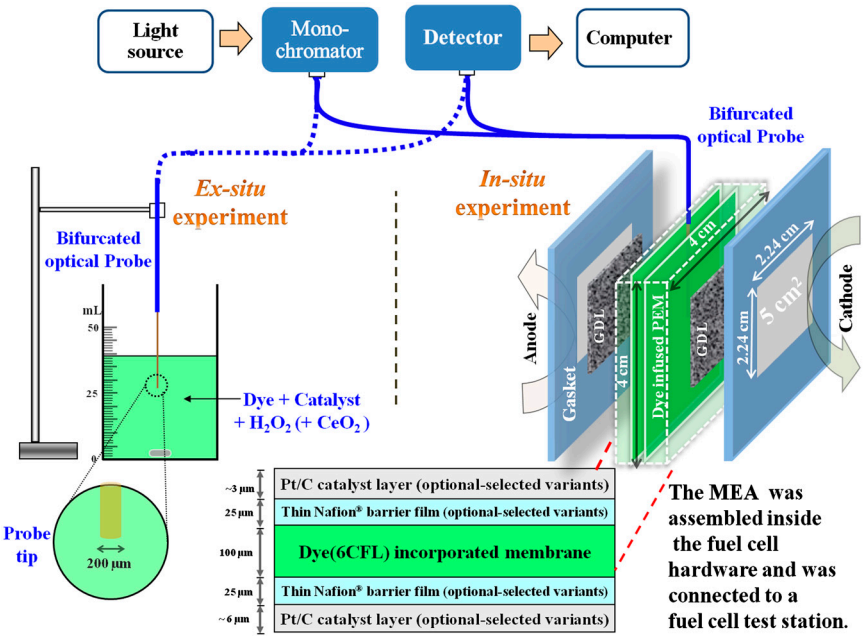

Fig. 1. Setup for ex situ and in situ fluorescence experiments.

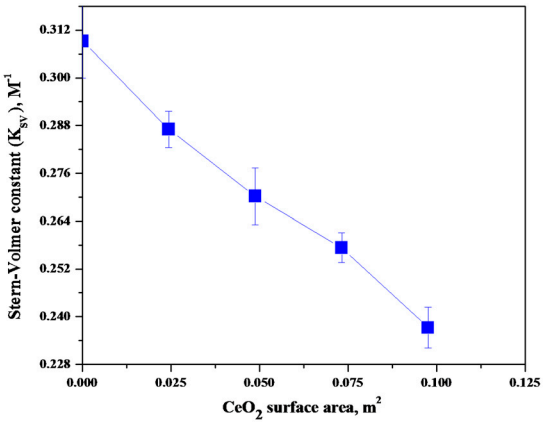

Fig. 3. Stern-Volmer constants as a function of the total surface area of CeO_2 present in the system.

change in Stern-Volmer constants (K_{SV}) as a function of the total surface area of CeO_2 nanoparticles present in the system. The drop in the Stern-Volmer constant with increasing total CeO_2 surface area, confirmed that CeO_2 acted as an effective FRS for hydroxyl and hydroperoxyl radicals.

However, it was shown through ex situ studies that the fluorescence response of FL was severely compromised in acidic environments. 6CFL was also assessed in acidic media and it was shown to have an adequate fluorescence response at low pH. Ex situ experiments were performed with 6CFL in the presence of Nafion® dispersed in 2-propanol. Nafion® dispersion added to the reactor lowered the pH of the solution to between 1 and 2. The fluorescence response of 6CFL decreased as the pH was lowered, but the observed signal intensity was sufficiently strong to clearly quantify the decrease in fluorescence response upon the addition of quencher. To explore the influence of pH on the fluorescence signal, the Nafion® dispersion was added to the reactor and then it was neutralized by titrating the solution with sodium hydroxide. The fluorescence signal of the probe in the presence of neutralized Nafion® dispersion was similar to values obtained with neutral aqueous solutions. The fluorescence response of 6CFL and FL were reduced at low pH because the carboxylic functional group(s) found in these molecular probes were protonated; consequently, the probes' molar absorptivity coefficient across the UV-Vis spectrum was reduced. See *SI Text*, p. 6. 6CFL was substituted for FL in all subsequent experiments as the fluorescence intensity of FL was reduced to almost zero in pH environments between zero and one. The results obtained from these ex situ experiments suggested that of the two molecular probes evaluated, FL and 6CFL, 6CFL would be more effective in acidic environments of the Nafion® membrane, which is at about pH 1 during fuel cell operation.

In Situ Fluorescence Experiments. In the next series of experiments, 6CFL was incorporated into the Nafion® membrane by dissolving 6CFL into the Nafion® dispersion. The 6CFL-Nafion® mixture was converted to a thin-membrane by casting onto a glass plate and evaporating the solvent. The dye-infused membrane, in selected cases, was transformed into a membrane electrode assembly (MEA) by the application of a carbon supported platinum catalyst layer on each side (MEA active area used was 5 cm^2). The dye-infused membranes, both with and without added catalyst layers, were prepared with a custom-made miniature bifurcated optical probe (200 μm diameter) placed in the center of two membranes that sandwiched it. The two membranes sandwiching the shaft of the miniature bifurcated probed had a total measured thickness of 300 μm (200 μm due to the diameter of the probe and 50 μm due to the thickness of each membrane). However, the two membranes sandwiched together below the sandwiched bifurcated probe had a total measured thickness of 100 μm. Thus, the thickness of the membrane used to determine the volume being probed inside the fuel cell was taken to be 100 μm. This bifurcated optical probe provided a conduit for both the incident light used to excite the molecular probe and the resultant fluorescence response. The membranes tested, with or without added electrodes, were sandwiched between carbon gas diffusion layers (GDLs), assembled into a fuel cell test hardware and sealed. The bifurcated optical fiber probe was connected to a monochromator that had a computer-controlled continuous wave xenon light source fed into it. The bifurcated probe was also connected to a photo diode array CCD detector. See Fig. 1. Further details describing the experimental setup used for in situ studies, preparing the dye-infused membranes, and preparing MEAs are presented under *SI Text*, pp. 2 and 3.

All in situ experiments were performed under the following conditions (unless otherwise noted): 80 °C cell temperature, 100% relative humidity of inlet gases, atmospheric pressure operation, gas flow rates of 0.1 liter per minute (lpm), and no external load. Initial in situ experiments were performed using the membranes without catalyst layer, wherein the carbon layers in the microporous layer of the GDL served as the sole catalytic sites for the production of hydrogen peroxide. It was expected that the degradation process during these in situ experiments would occur over several hours; therefore, it was important to ensure that the 6-CFL molecular probe was stable under elevated temperatures and high humidities for an extended period of time. To assess stability, humidified nitrogen gas was passed along both GDLs (N_2/N_2 operation) at 0.1 lpm and the in situ fluorescence response was continuously monitored. This experiment was performed at various temperatures (25 °C, 40 °C, 60 °C, and 80 °C). Experimental results confirmed the stability of the fluorescence response emanating from within the PEM. Tests were also executed with H_2/N_2 and N_2/O_2 combinations at the anode and cathode, respectively. Gases were passed in the following order: N_2/N_2, H_2/N_2, N_2/N_2, N_2/O_2, and N_2/N_2, and the in situ fluorescence response was monitored continually as a function of time. The results obtained are shown in Fig. 4. In all the above experiments, 6CFL demonstrated excellent stability in terms of its fluorescence response. In conjunction with ex situ results demonstrating the stability of 6CFL in the presence of stand-alone H_2O_2, these results suggested that the in situ fluorescence response of this probe would be sensitive and selective towards free radical ROS. After the stability of the molecular probe was verified under high temperature and high humidity conditions, H_2 and O_2 were fed into the fuel cell simultaneously. During this experiment, the gases diffused at a low, but finite rate, across the membrane leading to intermixing at each electrode. The gas crossover led to the formation of traces of H_2O_2, which in turn resulted in the formation of free radical

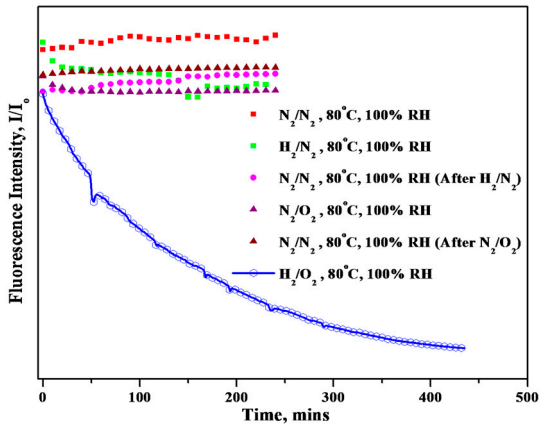

Fig. 4. Effect of different gases on the in situ fluorescence response of 6CFL contained within the PEM.

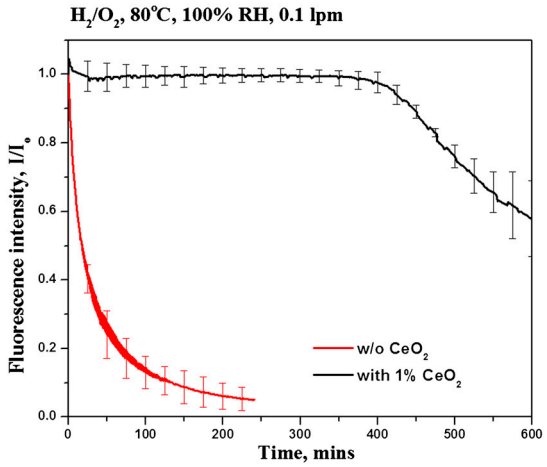

Fig. 5. Evidence of free radical scavenging activity of CeO_2 (membrane without catalyst layers).

ROS. For membranes without added platinum on carbon catalyst layers, the formation of H_2O_2 was catalyzed by carbon present in the GDL. Carbon has been reported to be an excellent catalyst for H_2O_2 formation (38). Fig. 4 shows the observed drop in the in situ fluorescence response as a function of time on stream in H_2/O_2 mode for membranes (without added catalyst layers). The observed first-order exponential decay of the fluorescence response confirmed the formation of ROS within the PEM and also demonstrated the suitability of this method to monitor ROS formation in situ in an operating fuel cell.

In Situ Fluorescence Experiments with CeO_2 as FRS. To assess the feasibility of using cerium oxide as a FRS, an identical experiment was performed where the membrane contained 1 wt% of CeO_2 nanoparticles. The addition of CeO_2 had a pronounced effect on the rate of ROS generation as indicated by the reduced rate of decay in the in situ fluorescence response on passing of H_2/O_2 (Fig. 5). The fluorescence response remained steady after the introduction of H_2 and O_2 into the fuel cell for over 7 h, demonstrating that the CeO_2 efficiently scavenged ROS within the PEM during this time-period. Subsequently, the fluorescence response decayed exponentially, but at approximately half the rate observed in membranes that did not contain CeO_2. The observed drop in fluorescence after 8 h in the CeO_2-containing membranes was attributed to a combination of the following factors: (*i*) the CeO_2 nanoparticles were not attached or tethered to the membrane and hence their mobility was not restricted, leading to leaching of CeO_2 particles out of the hydrated and swollen membrane, and consequently to diminished ROS scavenging ability, (*ii*) the large amount of oxygen species formed during ROS capture by CeO_2 (see Fig. 2) could hinder the CeO_2 scavenging ability by saturating oxygen vacancies on the CeO_2 surface, thereby compromising its regenerative nature, (*iii*) the degradation products of fluorescence dye or Nafion® could poison the CeO_2 active sites, again leading to a loss of ROS scavenging capacity. The immediate drop in fluorescence intensity observed after over 7 h of induction, as opposed to a gradual decrease from the beginning of the experiment, suggested that even a small amount of active CeO_2 nanoparticles was sufficient to effectively scavenge ROS within the PEM and that the added CeO_2 would function effectively to protect the PEM until a threshold (corresponding here to the abrupt onset of drop in fluorescence) was reached.

In Situ Fluorescence Experiments with Catalyst Layers. Subsequent to this proof-of-concept study, it was desired to evaluate the rate of ROS formation in membranes prepared with platinum on carbon based catalyst layers on each side (i.e., the conventional MEAs used in practice in fuel cell stacks). Initial in situ and ex situ experiments demonstrated that platinum nanoparticles in the catalyst layer interacted significantly with 6CFL, completely quenching its fluorescence response (see *SI Text*, p. 10 for details of the observed catalyst-dye interactions). Interaction of platinum with organic molecules, such as fluorescent dyes, have been widely reported in the literature (39–41). To alleviate this problem, a barrier layer was employed. The platinum on carbon catalyst was painted onto one side of two separate Nafion® NRE 211 films. A cast Nafion® membrane infused with 6CFL dye and containing an already imbedded bifurcated probe was sandwiched between the two Nafion® NRE 211 membranes such that the catalyst-coated layers faced outwards. In this configuration, the catalyst layers did not directly contact the 6CFL dye. See Fig. 1. The three films were hot pressed together, yielding a trilayer MEA. By creating a barrier between the membrane infused with 6CFL and the platinum nanoparticles, it was hypothesized that the metal-dye interaction would be significantly reduced. However, this trilayer MEA was still subject to a strong interaction between the dye and platinum particles during operation at 100% relative humidity. The interaction between the dye and platinum particles was made possible by the transport of the dye molecules toward the electrode layers through the condensed water phase in the membrane layers. To avoid this phenomenon, experiments were carried out at 50% relative humidity. Under these drier conditions, it was observed that the catalyst-dye interactions were significantly retarded, though not completely eliminated. A decay in fluorescence intensity was observed in experiments performed with catalyzed membranes in N_2/N_2 mode due to residual catalyst-dye interactions (Fig. 6*A*). To account for this independent source of decay in fluorescence, the data obtained from catalyzed membranes in H_2/O_2 mode was corrected for the observed catalyst-dye interactions. The corrected data is presented in Fig. 6*B*. The equation used to correct the in situ fluorescence data is also reported in Fig. 6*B*.

A trilayer MEA with platinum on carbon electrodes operated in H_2/O_2 mode exhibited a rate of fluorescence response decay that was about ~60% less than a MEA that contained electrodes with no platinum. See Fig. 6*B*. The reduced rate of fluorescence decay in catalyzed membranes was attributed to the decomposition of generated H_2O_2 to water by the platinum catalyst and the concomitant drop in the amount of ROS generated (42).

In the next experiment, trilayer MEAs with platinum on carbon electrodes where the central dye-infused membrane contained 1 wt% of CeO_2 nanoparticles were examined. In this case, the rate of decay in fluorescence intensity observed was lower than the baseline experiments with catalyzed membranes, which again confirmed that the CeO_2 particles were successful in scavenging the generated ROS. Unlike with uncatalyzed membranes, the 7-h induction period to the onset of fluorescence decay was not seen (or, more accurately, could not be resolved), because of the unavoidable fluorescence intensity decay superimposed on all experiments due to catalyst-dye interactions. A simple physical model was developed for fitting the transient fluorescence decay of 6CFL in the presence of ROS. The decay of 6CFL is analogous to the rate of generation of ROS within the fuel cell. See *SI Text*, pp. 3–5 for details of this model and parameters estimated. The key findings from fitting the apparent reaction rate constant for the decay of 6CFL revealed that the apparent reaction rate constant was low because the concentration of ROS in the membrane was small. The model confirmed that the incorporation of CeO_2 into the membrane provided an eightfold reduction in the apparent reaction rate constant. The apparent CeO_2 scavenging ability was determined from the model (for both in situ and ex situ experiments). The CeO_2 scavenging ability per unit area was much larger in in situ experiments (conducted around pH 0 to 1) vs. ex situ experiments (conducted around pH ~ 7) because the regeneration of Ce^{3+} from Ce^{4+} and

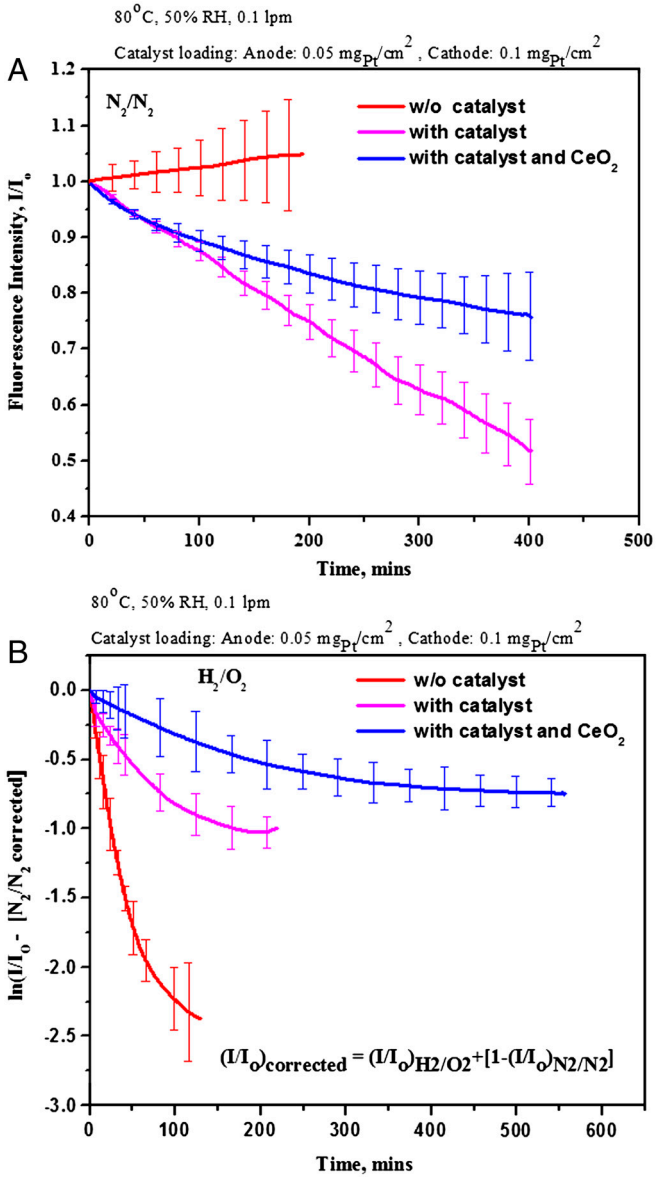

Fig. 6. In-situ fluorescence data obtained from dye incorporated Nafion® membranes (with and without catalyst layers *and* CeO_2) corrected for catalyst-dye interactions where appropriate (*A*) Experiment using N_2 across both electrodes. (*B*) Experiment using H_2 across the anode and O_2 across the cathode and corrected for metal-dye interactions using the N_2/N_2 data.

the concomitant regeneration of oxygen vacancies in the CeO_2 lattice are much more facile in acidic media.

Conclusions

This study demonstrates that an in situ fluorescence technique can be used for indirectly monitoring ROS formation during fuel cell operation. Additionally, this technique is useful for evaluating PEM degradation mitigation strategies-in this case, the technique has been used to demonstrate that CeO_2 nanoparticles incorporated into the PEM effectively scavenge free radical ROS. Ongoing and future work will focus on (*i*) identifying a molecular probe that is inert towards platinum while meeting other requirements listed in this paper. To this end, experiments assessing anthracene as a suitable molecular probe are underway; (43, 44) (*ii*) investigating the influence of fuel cell operating conditions on ROS generation rates. These conditions include: oxidant concentration, relative humidity, temperature, and electrode potential; and (*iii*) evaluating the efficacy of different FRS and alternate strategies in mitigating PEM degradation.

Materials and Methods

Chemicals Used. FL; fluka (analytical grade); 6CFL (Sigma Life Science, 97% HPLC); cobalt (II) nitrate hexahydrate (Aldrich, 98%); ammonium iron (II) sulfate hexahydrate (Sigma-Aldrich, 98%, Reagent Plus); hydrogen peroxide (ACROS, 35 wt% solution in water); 2-propanol (Sigma-Aldrich, 99%); Nafion® dispersion (5 wt% in 2-propanol); cerium (IV) oxide nano powder (Aldrich, 99.9%); hydrochloric acid (Aldrich, 0.975N solution in water); 0.1 N sodium hydroxide (Aldrich, ACS Reagent); DI water (prepared daily using a Direct-Q5 water filtration system by Millipore—18 MΩ); methanol (Fisher Scientific, ACS Reagent); platinum supported on carbon- Pt/C (40%) (Alfa-Aesar). All chemicals were used as received.

Fluorescence Equipment. Equipment manufacturer: Ocean Optics Inc.; light source: HPX-2000 CW (continuous wave) xenon lamp, 35 W, 185–2,000 nm; monochromator: Monoscan 2000, fiber optic scanning, 300–700 nm miniature bifurcated optical probe: custom-made –200 μm grating; detector: Jaz, CCD Detector (190 nm to 1,100 nm); and software: SpectraSuite.

In Situ and Ex Situ Fluorescence Spectroscopy Experiments. The in situ experiments presented in this paper were repeated three times for catalyzed and uncatalyzed membranes with and without CeO_2. The in situ experiments were repeatable, with acceptable variability as seen by the error bars in the data. The ex situ experimental data were also repeatable with the error bars in each case showing the variability associated with three experimental runs. Details describing in situ and ex situ fluorescence spectroscopy experiments are provided in the *SI Text* (pp. 1, 2, 8, and 9), as are details of preparation of membrane electrode assemblies and solutions for ex situ experiments. Dye-infused membranes with and without CeO_2 nanoparticles were prepared as follows:

Preparation of Membranes with 6CFL. 6 mL of 266 μM 6CFL (in 2-propanol) was added to 12 mL of 5% Nafion® solution and stirred for 8 h at 400 rpm. The resulting mixture was cast onto a 3.5 × 3.5 inch glass substrate. The cast solution was dried at 40 °C for 2 h. The membranes were subsequently peeled off and stored prior to use.

Preparation of Membranes with 6CFL and CeO_2 Nanoparticles. The procedure described above was followed, with 1 wt% of CeO_2 nanoparticles mixed into the casting solution.

Details about the volume of membrane probed, the spatial resolution of the measurement, and the transient response time of the spectrometer are elucidated under *SI Text*, pp. 2–5.

ACKNOWLEDGMENTS. The authors acknowledge National Science Foundation for funding. NSF Award # 0756473; PI V.R.

1. Collier A, Wang H, Yuan XZ, Zhang J, Wilkinson DP (2006) Degradation of polymer electrolyte membranes. *Int J Hydrogen Energ* 31:1838–1854.
2. Qiao J, Saito M, Hayamizu K, Okada T (2006) Degradation of perfluorinated ionomer membranes for PEM fuel cells during processing with H2O2. *J Electrochem Soc* 153: A967–A974.
3. Young AP, Stumper J, Knights S, Gyenge E (2010) Ionomer degradation in polymer electrolyte membrane fuel cells. *J Electrochem Soc* 157:B425–B436.
4. Healy J, et al. (2005) Aspects of the chemical degradation of PFSA ionomers used in PEM fuel cells. *Fuel Cells* 5:302–308.
5. Coms FD (2008) The chemistry of fuel cell membrane chemical degradation. *ECS Transactions* 16:235–255.
6. Borup RL, Mukundan R (2010) PEM fuel cell degradation. *ECS Transactions* 33:17–26.
7. Shah AA, Ralph TR, Walsh FC (2009) Modeling and simulation of the degradation of perfluorinated ion-exchange membranes in PEM fuel cells. *J Electrochem Soc* 156: B465–B484.
8. de BFA, Dam VAT, Janssen GJM (2008) Review: durability and degradation issues of PEM fuel cell components. *Fuel Cells* 8:3–22.
9. Walling C (1975) Fenton's reagent revisited. *Acc Chem Res* 8:125–131.
10. Woodmansee AN, Imlay JA (2002) Reduced flavins promote oxidative dna damage in non-respiring *Escherichia coli* by delivering electrons to intracellular free iron. *J Biol Chem* 277:34055–34066.
11. LaConti AB, Hamdan M, McDonald RC (2003) *Handbook of Fuel Cells* (Wiley-VCH, New York) p 647.

12. Gubler L, Dockheer SM, Koppenol WH (2011) Radical (HOO.bul., H.bul. and HOO.bul.) formation and ionomer degradation in polymer electrolyte fuel cells. *J Electrochem Soc* 158:B755–B769.
13. Schiraldi DA (2006) Perfluorinated polymer electrolyte membrane durability. *Polym Rev* 46:315–327.
14. Curtin DE, Lousenberg RD, Henry TJ, Tangeman PC, Tisack ME (2004) Advanced materials for improved PEMFC performance and life. *J Power Sources* 131:41–48.
15. Mittal VO, Kunz HR, Fenton JM (2006) Is H_2O_2 involved in the membrane degradation mechanism in PEMFC? *Electrochem Solid St* 9:A299–A302.
16. Chen C, Levitin G, Hess DW, Fuller TF (2007) XPS investigation of Nafion membrane degradation. *J Power Sources* 169:288–295.
17. Sies H (1993) Strategies of antioxidant defense. *Eur J Biochem* 215:213–219.
18. Bosnjakovic A, Schlick S (2004) Nafion perfluorinated membranes treated in Fenton media: radical species detected by ESR spectroscopy. *J Phys Chem B* 108:4332–4337.
19. Trogadas P, Parrondo J, Ramani V (2008) Degradation mitigation in polymer electrolyte membranes using cerium oxide as a regenerative free-radical scavenger. *Electrochem Solid St* 11:B113–B116.
20. Zhou C, Savant D, Ghassemi H, Schiraldi DA, Zawodzinski TA, Jr (2009) Membrane: life-limiting considerations. *Encyclopedia of Electrochemical Power Sources* 755–763.
21. Panchenko A, et al. (2004) In-situ spin trap electron paramagnetic resonance study of fuel cell processes. *Phys Chem Chem Phys* 6:2891–2894.
22. Panchenko A, Dilger H, Moller E, Sixt T, Roduner E (2004) In situ EPR investigation of polymer electrolyte membrane degradation in fuel cell applications. *J Power Sources* 127:325–330.
23. Bosnjakovic A, Kadirov MK, Schlick S (2007) Using ESR spectroscopy to study radical intermediates in proton-exchange membranes exposed to oxygen radicals. *Res Chem Intermediat* 33:677–687.
24. Fang X, Shen PK, Song S, Stergiopoulos V, Tsiakaras P (2009) Degradation of perfluorinated sulfonic acid films: an in-situ infrared spectro-electrochemical study. *Polym Degrad Stabil* 94:1707–1713.
25. Newton GL, Milligan JR (2006) Fluorescence detection of hydroxyl radicals. *Radiat Phys Chem* 75:473–478.
26. Gomes A, Fernandes E, Lima JLFC (2005) Fluorescence probes used for detection of reactive oxygen species. *J Biochem Biophys Methods* 65:45–80.
27. Ou B, et al. (2002) Novel fluorometric assay for hydroxyl radical prevention capacity using fluorescein as the probe. *J Agric Food Chem* 50:2772–2777.
28. Ou B, Hampsch-Woodill M, Prior RL (2001) Development and validation of an improved oxygen radical absorbance capacity assay using fluorescein as the fluorescent probe. *J Agric Food Chem* 49:4619–4626.
29. Naughton DP, Grootveld M, Blake DR, Guestrin HR, Narayanaswamy R (1993) An optical hydroxyl radical sensor. *Biosens Bioelectron* 8:325–329.
30. Liu W, Zuckerbrod D (2005) In situ detection of hydrogen peroxide in PEM fuel cells. *J Electrochem Soc* 152:A1165–A1170.
31. Kruczala K, et al. (2008) Spectroscopic investigations into degradation of polymer membranes for fuel cells applications. *Spectrochimica Acta A* 69:1337–1343.
32. Patil YP, Seery TAP, Shaw MT, Parnas RS (2005) In situ water sensing in a nafion membrane by fluorescence spectroscopy. *Ind Eng Chem Res* 44:6141–6147.
33. Naguib YMA (2000) A fluorometric method for measurement of oxygen radical-scavenging activity of water-soluble antioxidants. *Anal Biochem* 284:93–98.
34. Makrigiorgos GM, Kassis AI, Mahmood A, Bump EA, Savvides P (1996) Novel fluorescein-based flow-cytometric method for detection of lipid peroxidation. *Free Radical Biol Med* 22:93–100.
35. Babu S, Velez A, Wozniak K, Szydlowska J, Seal S (2007) Electron paramagnetic study on radical scavenging properties of ceria nanoparticles. *Chem Phys Lett* 442:405–408.
36. Sworski TJ, Mahlman HA, Matthews RW (1971) Reduction of cerium(IV) by hydrogen peroxide. Dependence of reaction rate on Hammett's acidity function. *J Phys Chem* 75:250–255.
37. Czapski G, Bielski BHJ, Sutin N (1963) The kinetics of the oxidation of hydrogen peroxide by cerium(IV). *J Phys Chem* 67:201–203.
38. Sljukic B, Banks CE, Mentus S, Compton RG (2004) Modification of carbon electrodes for oxygen reduction and hydrogen peroxide formation: The search for stable and efficient sonoelectrocatalysts. *Phys Chem Chem Phys* 6:992–997.
39. Bhowmick S, Saini S, Shenoy VB, Bagchi B (2006) Resonance energy transfer from a fluorescent dye to a metal nanoparticle. *J Chem Phys* 125:181102/181101–181102/181106.
40. Molenaar C, Teuben J-M, Heetebrij RJ, Tanke HJ, Reedijk J (2000) New insights in the cellular processing of platinum antitumor compounds, using fluorophore-labeled platinum complexes and digital fluorescence microscopy. *J Biol Inorg Chem* 5:655–665.
41. Lakowicz JR, Gryczynski I, Gryczynski Z, Dattelbaum JD (1999) Anisotropy-based sensing with reference fluorophores. *Anal Biochem* 267:397–405.
42. Antoine O, Durand R (2000) RRDE study of oxygen reduction on Pt nanoparticles inside Nafion: H_2O_2 production in PEMFC cathode conditions. *J Appl Electrochem* 30:839–844.
43. Sivanandan K, Aathimanikandan SV, Arges CG, Bardeen CJ, Thayumanavan S (2005) Probing Every Layer in Dendrons. *J Am Chem Soc* 127:2020–2021.
44. Aathimanikandan SV, Sandanaraj BS, Arges CG, Bardeen CJ, Thayumanavan S (2005) Effect of guest molecule flexibility on access to dendritic interiors. *Org Lett* 7:2809–2812.